Distal Femur Segmentation on MR Images Using Random Forests

Fabian Balsiger, Tiziano Ronchetti, and Martin Pletscher

***Abstract*—Segmentation of the distal femur from magnetic resonance (MR) images plays a crucial role in clinical practice. Diagnosis, disease progression monitoring, preoperative planning, and treatment analysis of diseases like osteoarthritis are applications. We developed a fully automatic method to segment the distal femur on MR images. Our method uses random forests (RF) and consists of two main phases: training and segmentation, i.e., a RF model is trained that enables RF voting to classify the distal femur on MR images. We evaluated our method with 20 MR data sets manually labeled by experts. A leave-one-out cross-validation was performed ($n = 10$) and Dice similarity coefficients (DSC) were obtained. The mean DSC is 92.37 ± 0.0266. Mean sensitivity is 91.57% and mean specificity is 99.29%. Training the RF model with 19 data sets took in average 791 seconds and segmenting an image 45 seconds ($n = 200$). Our method is suitable to segment the distal femur with high accuracy and precision. Moreover, the duration to segment the femur with less than a minute is feasible for clinical use.**

***Index Terms*—Fully automated femur segmentation, femur detection, segmentation, random forest (RF), magnetic resonance imaging (MRI).**

I. Introduction

SEGMENTATION of the distal femur from magnetic resonance (MR) images plays an important role in diagnosis, disease progression monitoring, preoperative planning, and treatment analysis of diseases like osteoarthritis (OA). OA is a disabling disease, affecting more than one third of the population over the age of 60. Monitoring the progression of OA or the response to structure modifying drugs requires exact quantification of the knee cartilage by measuring, e.g., the bone interface, the cartilage thickness or the cartilage volume [1]. Manual delineation for detailed assessment of knee bones and cartilage morphology, as it is often performed in clinical routine, is generally irreproducible and labor intensive with reconstruction times up to several hours [2]. The demand for automatic segmentation of knee bone and cartilage tissue is growing due to increasing availability of magnetic resonance imaging (MRI) scanners. MRI has the distinct advantage that it can delineate knee cartilage perceivably.

Therefore, our aim was to develop a fully automatic method to reduce segmentation time from hours to minutes and increase the robustness of the segmentation. In this paper we present **RF**em**IA** (**R**andom **F**orest **Fem**ur **I**mage **A**nalysis), an innovative platform to segment the distal femur on MR images.

The authors are students at the department of Biomedical Engineering, University of Bern, Switzerland. Use e-mails fabian.balsiger@students.unibe.ch and martin.pletscher@students.unibe.ch to contact F. Balsiger and M. Pletscher, respectively. T. Ronchetti can be contacted under tiziano.ronchetti@bfh.ch.

Manuscript received January 8, 2016.

Our method is based on random forest (RF) voting. RFs describe an ensemble of decision trees trained independently on a randomized selection of features. They are well suited to classification, regression, and other problems [3]. The use of RFs in medical image segmentation is relatively new but they have showed a wide range of applications with reasonable performance. Applications include e.g., delineation of the myocardium in adult 3D-echocardiography [4], classification of the brain tissues on MR images [5], and segmentation of multiple sclerosis in multichannel brain MR images [6]. Various approaches to improve the performance of traditional RF have been proposed lately. Yaqub et al. [7] used a feature selection method which learns a distribution of good features at each level of the trees. Consideration has also previously been given to proposing weighting schemes to weight the decision of each tree in the forest [8], [9]. Comparison with traditional RF showed enhanced accuracy for both approaches.

The following section begins with a review of related work and the state-of-the-art methods regarding the segmentation of the distal femur. We then introduce our method and describe the used materials, followed by the presentation of the obtained results. Last, we discuss our method and results and give a conclusion.

II. Related Work

The segmentation of the distal femur, or more broadly the segmentation of the knee bones and its cartilages, has been addressed by different authors. In 2010 a challenge was conducted at the Medical Image Analysis for the Clinic: A Grand Challenge workshop at the Medical Image Computing and Computer Assisted Intervention (MICCAI) conference in Beijing, China [10]. Results from 19 teams are published on the challenge's website [1].

An approach for segmentation the articular cartilage based on supervised learning was presented in [11], where an evaluation on 46 MRI data sets with no or mild OA resulted in an average Dice similarity coefficient (DSC) of 0.80, a sensitivity of 90.0% and specificity of 99.8%. A similar approach in combination with an elastic registration scheme was presented in [12] but only evaluated on a single MRI data set.

Fitting of a probabilistic atlas to MRI data, exploiting linear programming, was presented in [13] to segment the cartilage of the patella, achieving high DSC's. Fripp et al. [14], used statistical shape models (SSM) to extract the bone-cartilage interface (BCI). 20 MRI data sets from healthy subjects were segmented with DSC's of 0.96, 0.96 and 0.89 for the femur,

[1] http://www.ski10.org

the tibia and the patella, respectively. An average point-to-surface error of $0.16mm$ on the BCI.

A multi-object graph-based approach to segment the bones and the cartilage of the knee with minor manual interaction (approximately 30 sec) was proposed in [15]. An evaluation on 16 MRI data sets showed average surface positioning errors of $0.2mm$ to $0.3mm$ for the bones and $0.5mm$ to $0.8mm$ for the cartilage.

Comparing the performance of these different approaches is difficult, because evaluation results strongly depend on varying properties and origins of the employed image data (e.g., MR sequences, varying types of pathologies) as well as different evaluation metrics.

III. Materials & Method

In this section we first give an overview of the used materials and second introduce our method for the segmentation of the distal femur on MR images.

A. Materials

We used 20 MRI data sets of the human knee to validate the proposed method and compared it with other state-of-the-art segmentation methods. The data sets consist of images with ground truth annotations of the femur, tibia, articular cartilage, and meniscal cartilage by clinical experts. The data set sizes are approximately $150\ x\ 180\ x\ 105$ voxels with $0.39\ x\ 0.39\ x\ 1\ mm^3$ voxel spacing.

The data sets have been acquired under standardized conditions. Thus, the pose of the femur in the images is roughly the same and therefore we can make assumptions about the position of the distal femur in the image.

Further information about the data sets such as gender, age, and medical condition were not available due to the anonymization of the data sets.

B. Method

Our fully automated method to segment the distal femur on MR images uses RF voting. The method consists of two phases: training and segmentation, i.e., a RF model is trained that enables RF voting to finally segment the femur. The complete segmentation pipeline with both phases is shown in Fig. 1. The steps in each phase are described in this section.

1) Pre-processing: The input data is identically pre-processed in both main phases of our segmentation pipeline. The aim is to equalize the image and to remove noise. The images are first normalized using z-score normalization [16]. Second, to remove noise and to improve the signal-to-noise ratio (SNR) slice-wise Wiener filtering is applied. Third, the cohesion of regions is improved by applying slice-wise median filtering.

2) RF Training: The core of our method is the RF model. The RF is trained with the data set each consisting of the pre-processed MR image and its corresponding label image. The built RF model is then used to obtain a segmentation of the femur by RF voting. Our RF model is built by bagged decision trees with 20 trees. We randomly choose 5% of the voxels that show femur and 5% of the non-femur voxels from each data set to train the RF. For each chosen voxel we then extract its features which are described more in detail below. The feature extraction is implemented as concurrent operation to reduce the computational time. Once the RF model is built it can be used to vote other data sets to obtain a segmentation of the femur (RF voting step). The features are therefore extracted for all voxels of the data set. Thus, the RF voting classifies each voxel as femur or non-femur which yields a segmentation.

We used the following features for the RF. In the below equations $v_{i,j,k}$ denotes the voxel at position i, j, k and $I\ x\ J\ x\ K$ refers to its volumetric neighborhood.

Spatial location: The spatial location of each voxel is normalized and directly used as feature since the position of the femur is roughly the same in all data sets.

Volumetric mean: The mean μ of the voxel intensity within its neighborhood is calculated by

$$\mu = \frac{1}{N} \sum_{i=-\frac{I}{2}}^{\frac{I}{2}} \sum_{j=-\frac{J}{2}}^{\frac{J}{2}} \sum_{k=-\frac{K}{2}}^{\frac{K}{2}} v_{i,j,k}, \tag{1}$$

where $N = I \cdot J \cdot K$.

Volumetric variance: The variance σ^2 of the voxel intensity within its neighborhood is given by

$$\sigma^2 = \frac{1}{N} \sum_{i=-\frac{I}{2}}^{\frac{I}{2}} \sum_{j=-\frac{J}{2}}^{\frac{J}{2}} \sum_{k=-\frac{K}{2}}^{\frac{K}{2}} (v_{i,j,k} - \mu)^2, \tag{2}$$

where $N = I \cdot J \cdot K$ and μ is the mean.

Volumetric entropy: The entropy E in the neighborhood of voxel v is given by

$$E = -\sum_{i=-\frac{I}{2}}^{\frac{I}{2}} \sum_{j=-\frac{J}{2}}^{\frac{J}{2}} \sum_{k=-\frac{K}{2}}^{\frac{K}{2}} p(v_{i,j,k}) \log(p(v_{i,j,k})), \tag{3}$$

where $p(v)$ is the probability that the difference between neighboring voxels of v is equal.

Skewness: The skewness s is computed slice-wise in a $3\ x\ 3$ neighborhood by

$$s = \frac{E(v-\mu)^3}{\sigma^3}, \tag{4}$$

where μ is the mean of v, σ is the standard deviation of v, and $E(t)$ represents the expected value of the quantity t.

Kurtosis: The kurtosis k in a $3\ x\ 3$ neighborhood is given by

$$k = \frac{E(v-\mu)^4}{\sigma^4}, \tag{5}$$

where μ is the mean of v, σ is the standard deviation of v, and $E(t)$ represents the expected value of the quantity t.

Canny edge: Canny edge detection filter [17] is used to extract edges from each slice of the data set.

Hessian: The Hessian H of each slice I is computed by

$$H = \begin{pmatrix} \frac{\partial^2 I}{\partial x^2} & \frac{\partial^2 I}{\partial x \partial y} \\ \frac{\partial^2 I}{\partial y \partial x} & \frac{\partial^2 I}{\partial y^2} \end{pmatrix}. \tag{6}$$

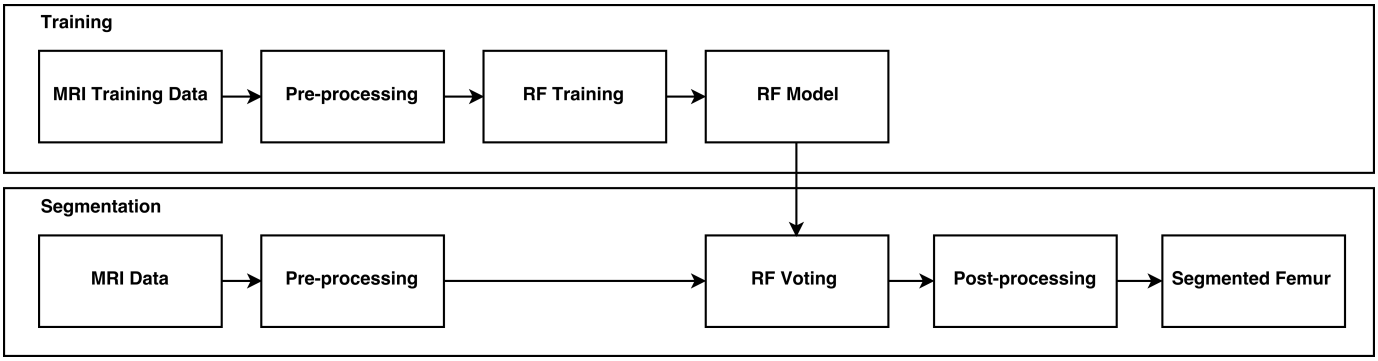

Fig. 1. The segmentation pipeline with the phases, training and segmentation. Each phase consists of separate steps to obtain the final segmentation of the distal femur. The reader is referred to the text for a detailed description on the separate steps.

3) Post-processing: The obtained segmentation from the RF voting step is then post-processed to achieve the final segmentation of the distal femur. The post-processing consists of morphological operations. We erode the segmentation, extract the largest connected volume, fill holes within areas, and finally dilate the segmentation to smooth the contour and remove artifacts at the border of the segmentation.

C. Evaluation Metrics

We evaluated our method using the DSC given by

$$Dice(A, B) = 2 * \frac{|A \cap B|}{|A| + |B|}, \tag{7}$$

where A is the segmentation result and B is the ground truth.

Moreover, sensitivity and specificity have been calculated for the segmentation.

IV. Results

This section presents results obtained by a leave-one-out cross-validation with the 20 data sets introduced previously. Furthermore, common segmentation issues are shown.

The cross-validation has been performed ten times. Both, DSC without and with post-processing were obtained. Sensitivity and specificity have been calculated. The method took in average 791 seconds ($n = 200$) for the training phase with 19 images. The segmentation phase for one data set took 45 seconds in average ($n = 200$)[2].

Fig. 2 shows box plots of the DSC for each data set obtained by the leave-one-out cross-validation ($n = 10$). The mean DSC is 0.9237 ± 0.0266. The median DSC is above 0.92 for 15 out of the 20 data sets. Five data sets have a median DSC below 0.90. The mean DSC without post-processing is 0.8921 ± 0.0372.

Table I summarizes the mean, median and standard deviation of the DSC, sensitivity, and specificity for each data set separately. It can be observed that the specificity is high for all data sets.

[2]Microsoft Windows 10 Education 64-bit (10.0, Build 10240) with MATLAB, 8.5.0.197613 (R2015a, 64-bit) from MathWorks, Inc. (Natick, MA; United States). Running on a 3.5 GHz Intel Core i5-4690 processor with 8 GB 1600 MHz DDR3 memory.

Fig. 3 shows a volume visualization of data set 11. This data set has the best DSC with 0.9528. The volume has been extracted by Delaunay tetrahedralization using the iso2mesh library [18]. MR image slices in each axis are shown for visual validation of the segmentation.

A. Common Segmentation Issues

Fig. 4 shows the segmentation of data set 2, the worst segmentation result, in the upper row and data set 11, the

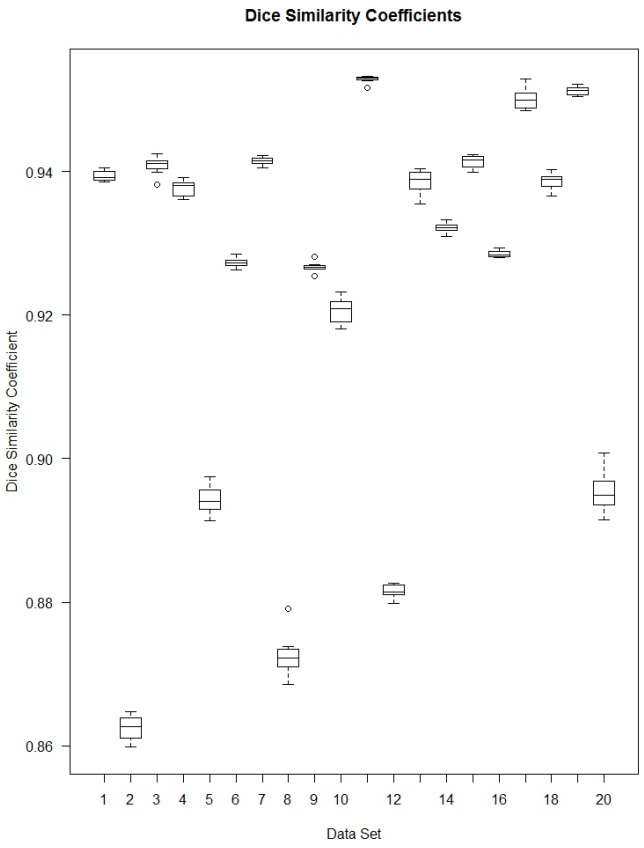

Fig. 2. Dice similarity coefficients (DSC) from the leave-one-out cross-validation for each data set ($n = 10$). The mean DSC over all data sets is 0.9237 ± 0.0266.

best segmentation result, in the lower row. Green indicates a correct segmentation, red indicates over-segmentation and blue indicates under-segmentation. Typical for all data sets are under-segmented areas at the first and last occurrences of the femur as in Fig. 4a and 4e. This bone-soft-tissue interface does also lead to under- and over-segmentation on other slices (refer to Fig. 4f, 4g, and 4h). Over-segmentation in the area of the femur's trunk towards its proximal end is another problem as it can be observed in Fig. 4b, 4c, and 4h. Besides invisible bone-soft-tissue interface this is probably caused due to MRI typical intensity inhomogeneities. Furthermore, heavily under-segmentation can be observed in Fig. 4c and 4d at the femur's trunk from data set 2. The raw data set does not show any special abnormalities on this slices. However, the femur contours are hard to determine even for humans.

TABLE I
RESULTS FROM THE LEAVE-ONE-OUT CROSS-VALIDATION. MEAN, STANDARD DEVIATION (SD) AND MEDIAN OF THE DICE SIMILARITY COEFFICIENT (DSC), SENSITIVITY AND SPECIFICITY OF THE SEGMENTATIONS ($n = 10$).

Data Set	Mean	SD	Median	Sensitivity	Specificity
1	0.9394	0.0007	0.9392	95.75%	99.12%
2	0.8625	0.0018	0.8626	80.39%	99.35%
3	0.9408	0.0013	0.9411	95.56%	99.22%
4	0.9377	0.0011	0.9381	94.58%	99.38%
5	0.8942	0.0020	0.8941	93.67%	98.26%
6	0.9273	0.0007	0.9273	90.94%	99.40%
7	0.9415	0.0006	0.9415	97.36%	98.99%
8	0.8726	0.0031	0.8722	82.11%	99.43%
9	0.9267	0.0007	0.9266	96.27%	98.76%
10	0.9206	0.0018	0.9209	86.94%	99.74%
11	0.9528	0.0005	0.9530	94.70%	99.51%
12	0.8815	0.0009	0.8815	94.49%	98.20%
13	0.9386	0.0016	0.9389	96.04%	98.98%
14	0.9322	0.0007	0.9322	89.28%	99.71%
15	0.9414	0.0010	0.9417	90.50%	99.74%
16	0.9285	0.0005	0.9284	87.64%	99.83%
17	0.9501	0.0015	0.9500	92.70%	99.64%
18	0.9386	0.0012	0.9389	95.76%	99.23%
19	0.9512	0.0006	0.9513	92.21%	99.75%
20	0.8954	0.0029	0.8949	84.43%	99.49%
Overall	0.9237	0.0266	0.9344	91.57 %	99.29 %

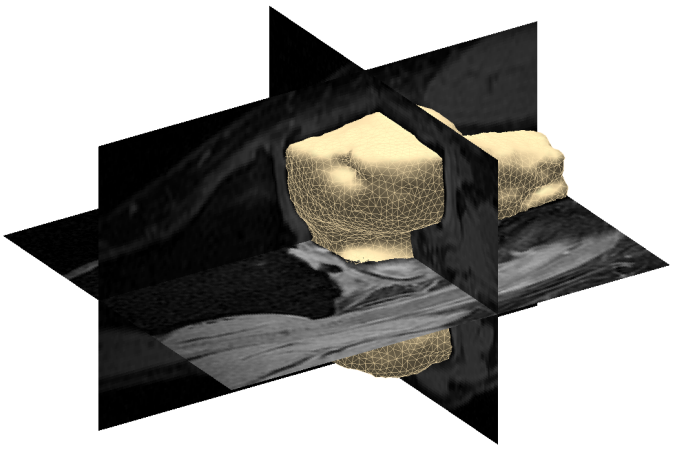

Fig. 3. Volume visualization of data set 11 with three slices. The segmentation yields a reasonable volume. (Best viewed in color)

V. DISCUSSION

In this section, we start by discussing the results we reported in Section IV and compare it to other authors. We then give a general discussion about RF as segmentation method for the distal femur. Last, we discuss possible future work and improvements.

A. Performance

Our method achieves a good performance when evaluated with the twenty data sets. Compared with the state of the research, we can say that we have achieved a first step in the direction of a competitive algorithm. Our mean DSC is to our knowledge solid but not yet in the same area as other scientific work. Refer to Table II for a comparison of our method to related work.

A limiting factor in the evaluation of our method is the manually segmented ground truth. We do not know about the quality of the ground truth. Poor ground truth can result in wrong evaluation measurements. One has also to consider that we have no knowledge about the data sets the other reported authors have used. Moreover, different evaluation metrics are used in the literature. Thus, comparison of results is not an easy task.

However, there is still room left for improvement. Five data sets have a median DSC below 0.90. The main segmentation issues, invisible bone-soft-tissue interfaces and MRI typical intensity inhomogeneities, seem to have a high impact on those data sets. Nevertheless, we could not finally reveal the cause to this worse outcome of those data sets compared to the other ones. Due to lack of knowledge about the origin of the data sets we could also not conclude on patient and data set specific properties. E.g., we could no examine the performance of mixed-gender and gender-specific models. However, Lindner et al. [20] conclude that a mixed-gender model performs well on their proximal femur segmentation.

Training and building the RF model is currently time consuming and not usable in clinical routine. Since there is no need to build the RF model newly for every segmentation and can be saved for later use, we do not consider this as a major drawback. The method is able to segment a data set in less than a minute using a precalculated RF model. This is fast and feasible for clinical use. Moreover, we believe that an improvement in terms of computation time can be achieved

TABLE II
COMPARISON OF DICE SIMILARITY COEFFICIENT (DSC) TO RELATED WORK.

Method	DSC
Fripp et al. 2007 [14]	0.96
Dam 2015 [19]	0.97
Our Method	0.9237

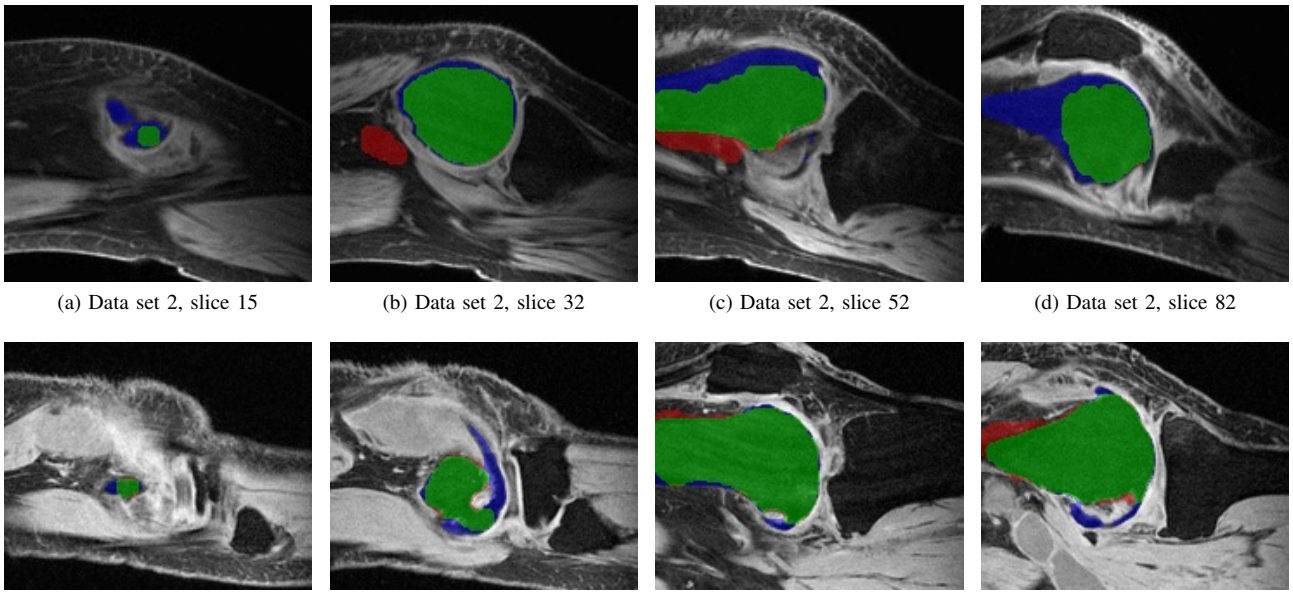

(a) Data set 2, slice 15 (b) Data set 2, slice 32 (c) Data set 2, slice 52 (d) Data set 2, slice 82

(e) Data set 11, slice 13 (f) Data set 11, slice 18 (g) Data set 11, slice 45 (h) Data set 11, slice 67

Fig. 4. Segmentation issues: Slices from the worst (data set 2, upper row) and the best segmented (data set 11, lower row) data sets are shown. Green indicates a correct segmentation, red indicates over-segmentation and blue indicates under-segmentation. Invisible bone-soft-tissue interfaces and intensity inhomogeneities typical for MRI are causes to the segmentation issues. (Best viewed in color)

for both the training and segmentation phases by optimizing the parameters and implementing the method in C++.

B. RF for Femur Segmentation

We have shown that an RF classifier trained with appropriate features is feasible to segment the distal femur on MR images. However, the mean DSC of 0.8921 without post-processing is not accurate enough and can not compete with results from other state-of-the-art methods. Crucial to achieve a good segmentation result with our method is the post-processing. Our morphological post-processing is adapted to the limitations of the RF model. Thus, we are able to increase the mean DSC by 0.0316 and simultaneously lower the standard deviation with post-processing.

In Appendix A, we present and discuss our choice of parameter used for the method and the evaluation. The method is generally insensitive to those parameters in terms of accuracy and precision. However, one can influence the computational effort significantly by adjusting the parameters.

We have tested other features in addition to those mentioned in Section III-B2. We performed an extensive evaluation of those features in various combinations. Although we included advanced features that play a relevant role in other research areas like computer vision (e.g., object recognition), none among those played an considerable role for our purpose. We conclude that the investigation of the role of features is an essential aspect when working with RF. We chose our features such that they yield a robust segmentation and to be as simple as possible to lower the computational effort.

C. Future Work

In future work the method could be enhanced to improve the segmentation by optimizing the RF training with more data sets. Moreover, many other features could be tested to find an advanced set of features that allow to improve the distinction between femur and other tissues present in the MR images. One could also introduce patient data such as gender, age, or medical condition to adapt the method accordingly. Further improvement could be achieved by incorporating images from different MRI modalities like T1, T2, or T1 flair. We believe this could help to distinct between bone and cartilage tissue greatly.

Our method does currently only segment the distal femur. Obviously, the method can be extended to segment the articular and meniscal cartilages and the proximal tibia. This could possibly lead to an increase in the DSC for the femur too.

Moreover, the method can be extended by statistical shape model (SSM) and active shape model (ASM). Work has been done in this area by other authors [14] and initial steps in this direction have already be implemented in combination with our method. First results look promising but are not stable enough to be presented.

VI. Conclusion

We presented **RF**em**IA** for the fully automatic segmentation of the distal femur on MR images using RF. The platform is feasible to segment the distal femur with high accuracy and precision. Further research and evaluation has to be done to increase the accuracy.

Appendix A
Choice of Parameters

The method is generally insensitive to most of the parameter settings. A change in the below introduced parameters does not affect the segmentation outcome significantly. However, it can

affect the computational effort to build the RF model and to segment an image.

A. Random Forest Parameters

Number of trees: The number of trees to train the RF has been determined by trial and error to be 20. Underfitting occurred with a number of trees lower than 20 in certain cases. More than 20 trees does not improve the DSC significantly and thus has no benefit.

Number of voxels: We used 5% of the voxels that show femur and 5% of the non-femur voxels from each data set to train the RF. Tests showed that the DSC does not improve significantly with increasing number of voxels used to train the RF. Though, the computational time is increased by factor 2.5 for each additional 5% voxels.

Volumetric neighborhood: We determined a neighborhood of $I\ x\ J\ x\ K = 5\ x\ 5\ x\ 3$ voxels for the volumetric features (i.e., mean, variance, and entropy) by trial and error. Tests showed that a smaller or larger neighborhood does negatively affect the RF voting outcome. A change in the neighborhood size does not significantly affect the computational effort.

B. Segmentation Parameters

Scaling factor: The image that is segmented was scaled to a smaller size to achieve a faster segmentation. A scaling by 0.5 has been determined for our evaluation. Segmentation without scaling does not improve the segmentation result significantly but does increase the computational time by factor 4.

ACKNOWLEDGMENT

The authors would like to thank Prof. Dr. Mauricio Reyes for his generous support and helpful feedback during the laboratory and for providing the materials. He gave us an excellent introduction to the field of random forests, statistical shape models, and active shape models.

REFERENCES

[1] H. Graichen, R. von Eisenhart-Rothe, T. Vogl, K.H. Englmeier, F. Eckstein, *Quantitative assessment of cartilage status in osteoarthritis by quantitative MRI: technical validation for use in analysis of cartilage volume and further morphologic parameters.* Arthritis and rheumatism, vol. 50, no. 3, March 2004, pp. 811-816.

[2] H. Shim, S. Chang, C. Tao, J.H. Wang, C.K. Kwoh, K.T. Bae: *Knee cartilage: efficient and reproducible segmentation on high-spatial-resolution MR images with the semi-automated graph-cut algorithm method.* Radiology, vol. 251, no. 2, May 2009, pp. 548-556.

[3] L. Breiman: *Random forests*, Mach. Learn., vol. 45, pp. 532, 2001.

[4] V. Lempitsky, M. Verhoek, J.A. Noble, and A. Blake, *Random forest classification for automatic delineation of myocardium in real-time 3-D echocardiography.* in Proceedings of the 5th International Conference on Functional Imaging and Modeling of the Heart. New York: Springer-Verlag, 2009.

[5] Z. Yi, A. Criminisi, J. Shotton, and A. Blake, *Discriminative,semantic segmentation of brain tissue in MR images.* Med. Image Comput. Comput. Assist. Intervent., vol. 12, 2009, pp. 558-565.

[6] E. Geremia, B. H. Menze, O. Clatz, E. Konukoglu, A. Criminisi, and N. Ayache, *Spatial decision forests for MS lesion segmentation in multi-channel MR images* in Proc. MICCAI, Beijing, vol. 13, 2010, pp. 111118.

[7] M. Yaqub , M. K. Javaid, C. Cooper, and J. A. Noble *Investigation of the role of feature selection and weigthed voting in random forests for 3D volumetric segmentation.* in IEEE Transactions on medical imaging, vol. 33, no. 2, Febr. 2014, pp. 258-271.

[8] M. Yaqub, P. Mahon, K. Javaid, C. Cooper, and A. Noble, *Weighted voting in 3-D random forest segmentation* in Med. Image Understand. Anal., Coventry, U.K., 2010.

[9] M. Yaqub, K. Javaid, C. Cooper, and A. Noble, *Efficient volumetric segmentation using 3-D fast-weighted random forests* in MICCAI workshop on Machine Learning in Medical Imaging, Toronto, Canada, vol. 7009, 2011, pp. 184192.

[10] T. Heimann, B. J. Morrison, M. A. Styner, M. Niethammer, S. K. Warfield: *Segmentation of Knee Images: A Grand Challenge*, 2010.

[11] J. Folkesson, E. Dam, O. F. Olsen, P. Pettersen, C. Christiansen: *Automatic segmentation of the articular cartilage in knee MRI using a hierarchical multi-class classification scheme.* In: International Conference on Medical Image Computing and Computer-Assisted Intervention MICCAI. vol. 8, 2005, pp. 327334.

[12] S. Warfield, M. Kaus, F. A. Jolesz, R. Kikinis: *Adaptive, template moderated, spatially varying statistical classification.* Medical Image Analysis 4(1), March 2000, pp. 4355.

[13] B. Glocker, N. Komodakis, N. Paragios, C. Glaser, G. Tziritas, N. Navab: *Primal/Dual Linear Programming and Statistical Atlases for Cartilage Segmentation.* MICCAI Lecture Notes in Computer Science, vol. 4792, 2007, pp. 536543.

[14] J. Fripp, S. Crozier, S. K. Warfield, S. Ourselin: *Automatic segmentation of the bone and extraction of the bone-cartilage interface from magnetic resonance images of the knee.* Phys Med Biol, vol. 52, no. 6, 2007, pp. 16171631.

[15] Y. Yin, X. Zhang, D. D. Anderson, T.D. Brown, C.V. Hofwegen, M. Sonka: *Simultaneous segmentation of the bone and cartilage surfaces of a knee joint in 3D.* SPIE, 2009.

[16] Kreyszig 1979, p880 eq(5)

[17] J. Canny, *A computational approach to edge detection* IEEE Transactions on Pattern Analysis and Machine Intelligence, vol. 8, no. 6, Nov. 1986, pp. 679-698.

[18] Iso2mesh.sourceforge.net, (2016): iso2mesh. Visited on 04. 01. 2016 at http://iso2mesh.sourceforge.net/cgi-bin/index.cgi.

[19] Erik B. Dam: *Validation of the KneeIQ segmentation framework on SKI10*, 2010

[20] C. Lindner, S. Thiagarajah, J. M. Wilkinson, G. A. Wallis, T. F. Cootes: *Fully Automatic Segmentation of the Proximal Femur Using Random Forest Regression Voting.* IEEE Transactions on Medical Imaging, vol. 32, no. 8, Aug. 2013, pp. 1462-72.